R. & M. No. 3499

MINISTRY OF TECHNOLOGY

AERONAUTICAL RESEARCH COUNCIL

REPORTS AND MEMORANDA

Low-Speed Measurements of Skin-Friction on a Slender Wing

By L. A. Wyatt and L. F. East

LONDON: HER MAJESTY'S STATIONERY OFFICE

1968

PRICE 12*s.* 6*d.* NET

Low-Speed Measurements of Skin-Friction on a Slender Wing

By L. A. Wyatt and L. F. East

Reports and Memoranda No. 3499*
February, 1966

Summary.

Extensive measurements have been made with surface pitot-tubes of the skin friction on the upper surface of a slender wing. The surface pitot-tubes took the form of razor-blade segments attached magnetically to the model. This new method of mounting improves on the conventional technique, particularly in coping with a flow whose direction changes with incidence.

The results confirmed that high levels of skin-friction are present beneath a leading-edge vortex. The spanwise distributions of skin-friction at different chordwise locations were correlated successfully at a given incidence. The sensitivity to yaw of surface pitot-tubes in areas of three-dimensional flow was found to agree with previous determinations in two-dimensional flow.

LIST OF CONTENTS

*Replaces R.A.E. Tech. Report No. 66 027 — A.R.C. 28 089.

1. *Introduction.*

The distribution of skin friction over a slender wing with established leading-edge vortices is of considerable intrinsic interest, but has only previously been determined at supersonic speed[1]. This Report describes comprehensive low-speed measurements of the skin-friction on the upper surface of a slender wing (rhombic cone) at incidence. Using two test speeds, the skin friction was determined at three chordwise stations for each incidence and then correlated in terms of a flat-plate skin-friction coefficient based on distance from the leading-edge apex. An attempt to correlate the spanwise distributions of skin friction taken at different incidences was only partially successful.

The experiments used a new version of the razor-blade technique for measuring skin friction[1,2]. The razor-blade segments were held on by small magnets set flush in the model surface, each magnet incorporating a pressure hole. Thus the segments could be easily rotated to cope with the variation in flow direction experienced at a fixed point over a range of incidence. Measurements were taken of the sensitivity of the derived skin friction to position of the razor-blade segment relative to the pressure hole. Tests were also made to relate the readings of surface pitot-tubes aligned (a) with the local surface-flow direction and (b) with the free-stream direction.

In a previous Report[3], skin-friction measurements were combined with values of the surface-pressure fluctuations and the relation between the quantities was interpreted provisionally as evidence favouring the hypothesis that the surface-pressure fluctuations in the three-dimensional region beneath a leading-edge vortex are generated by the same mechanism as in two-dimensional flow. It had been hoped that the results reported here, in conjunction with measurements of pressure fluctuations taken by Owen at the same time, would put the conclusions of Ref. 3 on a firmer footing. However, the pressure measurements revealed a real suspicion that the energy spectrum, particularly at high frequencies, extended beyond the range of the pressure transducers being used. Hence, any measured r.m.s. values would be misleading, particularly in the context of their correlation with skin friction. Moreover, it now seems that the above hypothesis for the origin of the pressure fluctuations under a vortex may be inadequate and that an appreciable contribution arises from an unsteadiness in the flow at the secondary separation line: further work is being undertaken by Owen to clarify the problem. The skin-friction measurements however are of sufficient interest in themselves to be described independently.

The experiments were conducted in the R.A.E. Bedford 13 ft × 9 ft low-speed wind tunnel.

2. *Experimental Details.*

2.1. *Model Details.*

The measurements were made on the upper surface of a rhombic cone of aspect ratio unity (leading-edge sweep 76 deg), whose cross-section had an included edge angle of 30 deg (*see* Fig. 1). The model was 6ft long and was pivoted in the tunnel about an axis just aft of the bluff base. The model was rigged inverted without a forward tare weight, thus yielding a completely clear upper (aerodynamic) surface. The model was of moulded fibre-glass construction.

For the skin-friction measurements, magnets incorporating static pressure holes were located on one half of the wing's upper surface in three spanwise rows at $x/c_0 = 0{\cdot}333$, $0{\cdot}554$ and $0{\cdot}777$. A total of 37 measuring points was provided, with the closest coverage in the region to be swept by the leading-edge vortex, i.e. outboard of $y/s_x = 0{\cdot}4$: the positions of the pressure holes are given in Table 1.

2.2. *Test Conditions.*

The experiments were carried out at nominal wind speeds of 150 and 250 ft/sec, giving Reynolds numbers based on root chord of $5{\cdot}7$ and $9{\cdot}5 \times 10^6$ respectively, and at incidences between 0 and 14 deg (uncorrected for constraint). Roughness in the form of grit (nominal size 0·004 in.) was applied to the upper surface of the wing at the apex as shown in Fig. 1. Under these conditions, the separated flow field at incidences of 6 deg and above was closely conical, except near the trailing edge, and the boundary layers were everywhere turbulent. At zero incidence, when no leading-edge vortex was formed, small areas of laminar and transitional flow were present near the wing leading-edge.

2.3. *Magnetic Mounting of Surface Pitot-tubes.*

With the exception of the method of securing the razor-blade segments to the surface, the surface pitot-tube technique did not differ from that used in previous experiments[3]. Most measurements were taken using a razor-blade height of 0·005 in. A few comparative values were taken using a blade height of 0·002 in. but these were more sensitive to blade position errors (*see* Section 2.6.). The surface pitot-tubes were aligned into the local surface flow direction with the aid of a surface flow pattern determined by the 'oil-flow' technique.

Previously[3], the small rectangular portions of razor blade were glued to the wing surface just overlapping the static pressure holes, and the razor-blade heights were measured using a travelling microscope at the end of the test period. This procedure was acceptable for a single determination at fixed incidence, but did not lend itself to the rapid completion of a series of tests at different incidences necessitating removal and re-alignment of the razor blades between each test. The process of cementing and aligning a total of 35 razor blades on the wing can occupy an hour, and the optical measurement of blade heights can take several hours, particularly if the blades have to be checked at several points along the leading-edge to confirm that they lie parallel to the wing surface within reasonable limits. Repetition of these processes would mean very inefficient use of available tunnel time.

The technique was therefore improved by setting small instrument magnets flush with the model surface to hold the razor-blade segments, which could then be set to any required direction. The time taken to place the segments into position is only a fraction of that needed to glue them down, e.g. under 10 minutes for 35 blades, and a series of tests can be done in quick succession. No time is taken up measuring blade height as this may be taken as half the blade thickness, which can be pre-determined quickly and accurately using a sensitive micrometer: only one determination is necessary. Care should be taken that the blade segments are flat, as distortion does occur occasionally whilst the segments are being cut to shape. Obviously, the magnet surface too must be flat and in a clean condition.

Instrument magnets are made from a hard and brittle alloy which can only be worked by grinding. However, the magnets are produced by a moulding technique and can incorporate a reasonably sized hole or cavity into which a static-pressure tapping can be inserted. For these tests, it was convenient to use a small cylindrical magnet* of 0·4 in. diameter and 0·4 in. depth with an off-centre hole of 0·11 in. diameter. On the advice of the manufacturers, the magnets were magnetized across a diameter to give the maximum adhesion for the blade segments. The mounting of a typical magnet/razor-blade combination is shown in Fig. 2. Before mounting in the model, a mild steel bush was inserted to half the depth of the hole in the magnet. After grinding the working surface of the magnet flat to a 30μ in. finish, a pressure hole of 0·030 in. diameter was drilled centrally through the bush and a 3/32 in. o.d. copper tube connection was cemented into the rear of the magnet (*see* Fig. 2). Each magnet was mounted with the pressure hole towards the free-stream direction. With a nominal blade size of 0·18 in. square, deviations of 45 deg in flow direction are possible before there is any risk of loss of adhesion due to the blade protruding over the edge of the magnet.

Some difficulty was experienced at first in flush mounting the magnets in the fibre-glass skin of the model to the desired accuracy. The following method was adopted finally. A clearance hole of about 0·5 in. diameter was drilled through the model skin (*see* Fig. 2) and a ground steel plate secured to the plane working surface across the face of the hole. The magnet (0·4 in. diameter) was inserted from the rear and adhered to the plate. Araldite was then run into the annular groove and allowed to set. After removing the ground plate, a little hand-finishing only was necessary to complete the flush mounting. By this means, it was possible to ensure that discrepancies in level near the edge of the magnet never exceeded 0·0002 in. this order of finish was felt desirable because the joints lay close to a razor-blade whose maximum height was only 0·005 in. An alternative approach of setting the magnets quite roughly into a cavity in the skin and grinding down the resulting composite surface was not so successful because of the differing hardnesses of the materials. The magnet tended to be left slightly proud with a depression in the surrounding adhesive. Recently, identical magnets have been mounted in a flat steel surface by sweating them into

*Type PM 198/0 produced by Murex Limited, Rainham, Essex.

position and grinding flat. However, a surround of magnetic material does seem to absorb some of the magnetic flux, thus decreasing the bond between magnet and blade segment.

Simple considerations show that, at test speeds of order 300 ft/sec, the maximum force tending to displace a razor-blade segment either along or normal to the surface is very small (of order 10^{-3} lb). No blade movement has been detected during tests. Recently, the identical model and magnetic mounting was tested successfully at supersonic speed.

2.4. *Razor-blade Calibration.*

The difference between the pressure recorded by a surface pitot-tube and the local static pressure is a calibrated function of the surface shear stress. The pressure difference Δp and the shear stress τ may be related as follows

$$\rho h^2 \tau/\mu^2 = C(\rho h^2 \Delta p/\mu^2)^m \tag{1}$$

where h is the height of the razor-blade leading-edge above the surface, and ρ and μ are respectively the air density and viscosity at the point of measurement. The values of C and m depend on the Mach number and on the state of the boundary layer, i.e. laminar or turbulent. Calibration data were obtained in a turbulent boundary layer on a flat plate with zero pressure gradient, using a Preston tube to define the skin friction[4]. Fig. 3 shows the calibration curve, including unpublished data obtained independently by Lovell and Owen. The data shows a slight systematic curvature, but, over the working range of the present tests, i.e. $10^3 < \rho h^2 \Delta p/\mu^2 < 10^5$, is closely represented by the following relation

$$\rho h^2 \tau/\mu^2 = 0{\cdot}29\,(\rho h^2 \Delta p/\mu^2)^{0{\cdot}76}\,. \tag{2}$$

The calibration (2) obtained in zero pressure gradient has been used to determine the skin friction in regions of three-dimensional flow with both favourable and unfavourable pressure gradients. The assumption implicit in this procedure is that, near the surface, the velocity profile of the turbulent boundary layer is determined solely by the shear stress at the wall and the properties of the fluid – hence the form of equation (1). It has in fact been possible to confirm that the chosen index m (= 0·76) is applicable in regions of pressure gradient. At an incidence of 12 deg, surface pitot-tube readings were taken at all the measuring points over the surface of the wing using two different razor-blade heights (h_1, h_2), and the ratio of the indicated pressure differences was found, i.e. $\Delta p_1/\Delta p_2$. At a fixed position with τ constant, equation (1) gives

$$m^{-1} = 1 + \frac{1}{2}\log(\Delta p_1/\Delta p_2)/\log(h_1/h_2)\,. \tag{3}$$

h_1 and h_2 were taken as 0·005 and 0·002 in. respectively. The derived values of m ranged between 0·72 and 0·79, with a mean value of 0·75. No consistent variation could be detected between values of m measured in positive or negative pressure gradients, and the mean value of 0·75 is taken as confirmation of the validity of the calibration (2) in regions of varying pressure. Some of the scatter in the individual values of m undoubtedly stemmed from difficulty in positioning the 0·002 in. razor-blades sufficiently precisely over the static pressure hole – evidence on this point is presented in Section 2.6.

Fig. 3 gives for comparison an unpublished subsonic calibration (M = 0·2) derived by the authors of Ref. 1. The index m has the same value 0·76, but the constant C is about 14 per cent larger. This is believed to be due to the differing section of the razor blades. Comparative tests at low speed have confirmed that grinding off the majority of the top half of the blades (as in Ref. 1) does in fact reduce the pressure difference recorded for a fixed shear stress, hence requiring a larger value for the constant C. Reductions in the abscissa ($\log_{10} \rho h^2 \Delta p/\mu^2$) of between 0·04 and 0·12 were observed, i.e. of the same order as the displacement of the two calibration lines. Although not important at supersonic speeds[1], the razor-blade section evidently needs to be specified precisely at subsonic speeds if inconsistencies of calibration are to be avoided.

2.5. *Accuracy of Skin-friction Measurements.*

The overall comparative accuracy of the skin-friction values is estimated to have an r.m.s. value of $\pm 2{\cdot}5$ per cent. This figure was obtained by repeating a set of readings at $\alpha = 12$ deg with the razor blades (0·005 in. high) inverted and replaced over the same static holes. In this way, errors due to the positioning of the razor blades, asymmetry of the blades and the measurement of the pressure difference were accounted for. A similar test with 0·002 in. razor blades gave a somewhat higher figure of $\pm 3{\cdot}8$ per cent. Comparison of skin-friction on values derived with the two blade heights indicated an r.m.s. error of $\pm 2{\cdot}8$ per cent: in this instance, calibration errors can contribute to the scatter. This experimental value of the likely accuracy compares well with the figure of about 6 per cent quoted in Ref. 3 where considerable inaccuracy arose in the determination of blade height. The absolute accuracy of the measurements is difficult to estimate conclusively and was not of primary concern. All the results presented in Section 3 were obtained using 0·005 in. blades, mainly because of their reduced susceptibility to error in position over the static hole.

2.6. *Position Error.*

In previous sections, mention has been made in passing of the uncertainty in blade calibration which can arise due to random errors in positioning the blade leading-edge immediately above the forward edge of the static hole. Fig. 4 shows the results of tests made with both 0·002 and 0·005 in. blades to detect the variation of the indicated skin friction with fore and aft position; unpublished values obtained by the authors of Ref. 1 are included also. The tests were made well inside the approximately two-dimensional flow region inboard of the vortex. The skin-friction C_{f_0} measured with the blade and hole leading edges coincident has been taken as the datum value and the index $m = 0{\cdot}76$ assumed to apply, i.e. $C_f/C_{f_0} = (\Delta p/\Delta p_0)^{0{\cdot}76}$. The results correlate well if the fore and aft displacement of the blade is expressed in terms of the blade height, rather than, for example, the static hole diameter. The blades are most sensitive to rearward movement, and casual positioning can easily introduce appreciable error, particularly with the 0·002 in. blades. A rearward displacement of 0·005 in. would lead to a 15 per cent reduction in the registered skin friction with a 0·002 in. blade – the error is reduced to 5 per cent with an 0·005 in. blade. The figures achieved for experimental accuracy (*see* Section 2.5.) suggest that, in practice, a positioning accuracy within $\pm 0{\cdot}002$ in. was being achieved. Nevertheless, some care is advisable (e.g. adequate lighting) to eliminate uncertainties.

3. *Discussion of Results.*

The results are presented initially in terms of the local skin-friction coefficient $C_f = \tau/q_0$, where q_0 is the free-stream kinetic pressure. Also used is a skin-friction coefficient C_{f_q} based on the local kinetic pressure q, i.e. $C_{f_q} = \tau/q = C_f/(1-C_p)$* where C_p is the local-pressure coefficient (uncorrected for blockage effects).

The oil flow technique was used to pick out the dominant features of the surface flow beneath the leading-edge vortex i.e. attachment line, inflexion line, etc. These flow features are identified with respect to the flow field of the vortex in the sketch included on Fig. 5. The oil flow patterns showed that, for $\alpha \geqslant 6$ deg, the spanwise positions of the flow features were independent of distance from the leading-edge apex showing that the surface flow was approximately conical. Fig. 5 shows the variation with incidence of the spanwise position of the various flow features. The positions of the attachment line, the inflexion line and the secondary and tertiary separation lines are shown as A, I, S and T respectively on the pressure distributions of Fig. 6 and on the skin-friction distributions of Fig. 8, 9 and 10.

The presence of a closely conical flow field was confirmed by the similarity at different x/c_0 of the spanwise pressure distributions, typical examples of which are presented in Fig. 6. Small chordwise

*Strictly speaking, $q/q_0 = [f(M_0)-C_p]/f(M)$, where $f(M) = 1+\frac{1}{4}M^2+0(M^4)$ and M, M_0 are respectively the local and freestream Mach numbers. In the present context, it is sufficiently accurate to take $q/q_0 = 1-C_p$ as in incompressible flow. The error involved is less than 3 per cent and tedious computation is avoided.

pressure gradients did however exist as shown in Fig. 7 which gives the chordwise pressure distribution near the centreline as a function of incidence. Full details of the measured pressure coefficients are given in Table 2.

3.1. *Skin-friction Measurements.*

Typical distributions of the skin-friction coefficient over the local semi-span are shown in Fig. 8 for $\alpha = 10$ deg: the full results are tabulated in Table 2. Moving outwards from the centreline, it can be seen that the skin friction rises steadily as the region swept by the leading-edge vortex is entered and reaches a peak value about twice that measured well inboard of the vortex. Beyond the peak, the skin friction falls to a minimum somewhat less than the level inboard of the vortex and subsequently rises as the leading-edge is approached.

Since conical flow is shown by the oil flow patterns to exist for angles of incidence of 6 deg and above, it should be possible to collapse the skin-friction distributions on to one curve for any particular incidence. To this end, it is reasonable to express the local skin-friction coefficient C_f in terms of a flat-plate skin-friction coefficient C_{f_x}, the representative length x being taken as the distance of the appropriate chordwise station from the leading-edge apex (*see* Fig. 1). The development of the boundary layer under the influence of a leading-edge vortex is clearly a complicated three-dimensional problem about which insufficient is known either to predict a theoretical form of C_f or to estimate the extent to which the above procedure may be expected to correlate the experimental values of C_f. However, the following argument may be used to indicate that in practice a reasonably close collapse of the results should be expected. It will be assumed that, so far as the skin friction is concerned, the difference between the development of a three-dimensional and a two-dimensional boundary layer can be represented by a progressive scaling of the development length. Thus, the effective Reynolds number of a three-dimensional flow is obtained by multiplying the Reynolds number based upon a suitable linear scale of the flow by a function of the pressure field through which the boundary layer has passed. In the present case the external flow is conical and so, ignoring chordwise pressure gradients due to incidence, the pressure field at constant incidence is completely defined by the value of y/s_x at which the skin friction is being measured and its scale is proportional to the value of x. Thus, the effective Reynolds number is taken as FR_x, where F is an unknown function of (y/s_x) and is considered to account for the integrated effect of the upstream pressure gradients through which the boundary layer has passed.

A suitable form for the flat-plate skin-friction coefficient C_{f_x} is[5]

$$C_{f_x} = 0{\cdot}288\,(\log_{10} R_x)^{-2{\cdot}45}. \tag{4}$$

Following the argument of the previous paragraph, it is proposed that the skin friction in the three-dimensional flow over the wing surface be represented by an extension of equation (4) as follows

$$C_f = 0{\cdot}288\,(\log_{10} F\,R_x)^{-2{\cdot}45},\ F = F(y/s_x) \tag{5}$$

Hence

$$\frac{C_f}{C_{f_x}} = \left(1+\frac{\log F}{\log R_x}\right)^{-2{\cdot}45}. \tag{6}$$

This implies that C_f/C_{f_x} is still a function of R_x. In the present experiments, $\log R_x$ varies between 6·3 and 6·8 whilst C_f/C_{f_x} varies between 0·8 and 3·0. From equation (6), it is readily seen that

$$\frac{d(C_f/C_{f_x})}{C_f/C_{f_x}} = 2.45\left[1-\left(\frac{C_f}{C_{f_x}}\right)^{-1/2{\cdot}45}\right]\frac{d(\log R_x)}{\log R_x}.$$

In this case, the variations in $\log R_x$ ($\pm$ 4 per cent) would give a maximum scatter in C_f/C_{f_x} of ± 6 per cent when C_f/C_{f_x} is 3·0.

The distributions of C_f/C_{f_x} obtained are shown in Fig. 9 and do exhibit a satisfactory collapse for the two velocities and three chordwise positions used. Much of the scatter that does exist can be attributed to the influence of the small chordwise pressure gradients (*see* Fig. 7). Near the model centreline, the pressure gradient is zero between 8 and 10 deg incidence, and these two incidences show the least scatter. At higher incidences, the pressure gradient is adverse and the value of C_f/C_{f_x} falls slightly with increasing x/c_0. The opposite tends to be true for incidence below 8 deg. At $\alpha = 0$ deg, it will be seen that C_f/C_{f_x} is discontinuous and clear evidence exists of some laminar flow near the leading-edge. In regions of laminar flow, the value of C_f/C_{f_x} will be in error since neither the calibration nor the estimate of C_{f_x} used is appropriate. At the lowest two incidences, the skin friction rises as $y/s_x \to 1$ because of the shorter boundary-layer runs involved. The skin friction beneath the leading-edge vortex rises to a peak value which exceeds that measured inboard of the vortex by a factor increasing progressively with incidence to a maximum of 2·5 for $\alpha \geqslant 10$ deg. At incidences of 6 deg and above, when the flow field is approximately conical, the inflexion line (I) corresponds closely with the maximum skin friction and the secondary separation line (S) with the minimum. Outboard of the minimum, the skin friction rises again near the leading-edge. The attachment and tertiary separation lines do not appear to correspond to any noteworthy characteristic of these curves.

The variation with incidence of the maxima and minima of Fig. 9 can be eliminated by basing the skin-friction coefficient on the local kinetic pressure q, giving C_{f_q}. The spanwise distributions of C_{f_q}/C_{f_x} are shown in Fig. 10. The mean value of $(C_{f_q}/C_{f_x})_{max}$ for the conical flow conditions ($\alpha \geqslant 6$ deg) is 1·7, and that for $(C_{f_q}/C_{f_x})_{min}$ is 0·6. C_{f_q}/C_{f_x} tends to unity on the model centreline, except at large incidences when presumably the size of the leading-edge vortices is such that they significantly influence the centre-line flow. It may well be fortuitous that the tertiary separation line appears now to correspond to C_{f_q}/C_{f_x} approximately equal to unity.

It would be most satisfying if the distributions of Fig. 10 could be combined to give a universal curve independent of incidence. Several typical lateral reference lengths could be used instead of the local semi-span s_x, e.g. the distance between any two of the attachment, inflexion and secondary separation lines. However, Fig. 10 shows that the inflexion point I does not correspond to the maximum value of C_{f_q}/C_{f_x} which, relative to that of C_f/C_{f_x} (Fig. 9), has moved slightly inboard and in effect upstream. The variation with incidence of the spanwise position of $(C_{f_q}/C_{f_x})_{max}$ is plotted on Fig. 5: clearly, its position relative to A, I, S and T varies with incidence, thus negating a universal curve.

3.2. *The Chordwise Component of Skin-friction.*

The experimental procedure used to measure the skin friction necessitates frequent entry into the tunnel and is not a practical proposition for large high speed tunnels. In such tunnels, the apparent chordwise component of the skin friction can be measured by pointing the razor blades permanently into the freestream direction with the advantage that all incidences can be treated consecutively without stopping the tunnel. To investigate whether or not this procedure is satisfactory, additional measurements were taken at $\alpha = 12$ deg with the razor blades set parallel to the model centreline.

The effect of yawing a razor-blade in a two-dimensional boundary layer has been investigated by Smith, Gaudet and Winter[1] who considered the following relationships

$$C_{f_\beta}/C_f = \cos\ \beta \tag{7}$$

$$\Delta p_\beta/\Delta p = \cos^2\beta \tag{8}$$

where Δp_β is the pressure difference recorded with the razor blade yawed through an angle β relative to the local surface-flow direction and C_{f_β} is the corresponding skin-friction coefficient calculated using the standard calibration (2). The latter expression (8) gave better agreement with experiment and seems intuitively more plausible than (7).

Fig. 11 shows the ratio of the apparent streamwise component of skin friction C_{f_β} to the true skin friction C_f at $\alpha = 12$ deg. Using either (7) or (8) to represent the behaviour of the yawed razor blade, the deviation β of the local flow from the freestream direction has been calculated. Equation (7) gives simply

$$\beta = \cos^{-1}(C_{f\beta}/C_f). \tag{9}$$

Using equation (8) and the calibration law (2), we find

$$\begin{aligned} \beta &= \cos^{-1}(\Delta p_\beta/\Delta p)^{\frac{1}{2}} \\ &= \cos^{-1}(C_{f\beta}/C_f)^{0\cdot658}. \end{aligned} \tag{10}$$

Equations (9) and (10) are plotted respectively as curves (1) and (2) in Fig. 11 and compared with direct measurements of β taken from an oil flow pattern. The measured β agrees well with that deduced from the skin-friction measurements using the relationship of equation (8). Thus the relationship governing the behaviour of a yawed razor blade in two-dimensional flow[1] appears to hold good in the three-dimensional flow field of the present experiment.

However, the above conclusion implies that a yawed razor blade does not measure the resolved component $C_f \cos\beta$ of the local skin friction. The ratio of the true to the apparent skin-friction component, i.e. $C_f \cos\beta/C_{f\beta}$ is given by equation (10) as $(\cos\beta)^{-0\cdot52}$ which amounts to 1·033 and 1·15 at yaw angles of 20 and 40 deg respectively. Consequently, appreciable errors would arise if, in a strongly three-dimensional flow field, the apparent shear stresses indicated by razor blades pointing in the freestream direction were integrated to give the skin-friction drag.

4. *Conclusions.*

At low subsonic speeds, the distribution of skin friction on the upper surface of a sharp-edged slender wing has been measured in detail over a wide range of incidence using the surface pitot-tube technique. Each surface pitot-tube was formed from a razor-blade segment attached to a magnet set flush in the model and incorporating a static pressure hole. This novel type of mounting simplifies the experimental procedure considerably and affords a valuable saving in testing time, particularly when dealing with regions of varying flow directions, e.g. beneath a leading-edge vortex.

At fixed incidence, the skin-friction distribution was obtained along three spanwise rows at two wind speeds and shows that beneath the leading-edge vortex the skin friction rises to a peak value of up to 2·5 times that measured inboard of the vortex. Outboard of this maximum the skin friction falls to a minimum at the secondary separation point and then rises again towards the leading-edge. The results are shown to correlate well in terms of a flat-plate skin-friction coefficient defined for a two-dimensional flow at a Reynolds number based on the distance x from the leading-edge apex of the wing. An attempt to collapse the results at different incidences was only partially successful.

Measurements taken in regions of highly three-dimensional flow with the surface pitot-tubes yawed relative to the local flow direction indicated that the sensitivity to yaw agreed well with existing evidence obtained in two-dimensional boundary layers. The results confirmed that a yawed surface pitot-tube does not measure the resolved component $C_f \cos\beta$ of the true skin friction, but more nearly $C_f \cos^{3/2}\beta$.

TABLE 1

Positions of Static Pressure Holes.

y/s_x		
$x/c_0 = 0{\cdot}333$	$x/c_0 = 0{\cdot}554$	$x/c_0 = 0{\cdot}777$
0·104	0·037	0·072
0·206	0·155	0·174
0·304	0·276	0·277
0·406	0·398	0·381
0·504	0·458	0·432
0·603	0·518	0·484
0·701	0·578	0·535
0·805	0·638	0·588
0·901	0·699	0·640
	0·758	0·691
	0·820	0·742
	0·880	0·795
	0·942	0·846
		0·897
		0·948

TABLE 2

Skin friction and Pressure Coefficients.

(a) 150 *ft/sec*

x/c_0	y/s_x	$\alpha = 0$ deg		$\alpha = 1$ deg		$\alpha = 2$ deg	
		$10^3\, C_f$	$+C_p$	$10^3\, C_f$	$+C_p$	$10^3\, C_f$	$+C_p$
0·333	0·104	2·9	0·034	2·9	0·026	3·0	0·012
	0·206	3·0	0·032	3·0	0·026	3·0	0·012
	0·304	3·1	0·035	3·0	0·027	3·1	0·015
	0·406	3·1	0·037	3·0	0·029	3·3	0·015
	0·504	3·5	0·037	3·4	0·031	3·3	0·016
	0·603	3·9	0·037	3·5	0·031	3·6	0·015
	0·701	4·0	0·040	3·8	0·031	4·0	0·015
	0·805	1·7	0·040	3·7	0·032	4·4	0·016
	0·901	2·2	0·045	4·4	0·035	4·2	−0·012
0·554	0·037	3·0	0·016	2·8	0·010	2·9	−0·002
	0·155	2·9	0·016	2·7	0·012	3·0	−0·002
	0·276	3·1	0·018	2·9	0·013	3·0	−0·002
	0·398	3·1	0·021	2·9	0·015	3·3	−0·002
	0·458	3·1	0·021	3·0	0·015	3·2	−0·001
	0·518	3·2	0·023	3·0	0·016	3·0	0·001
	0·578	3·0	0·024	2·9	0·016	3·4	0·001
	0·638	3·6	0·024	3·3	0·016	3·5	0·001
	0·699	3·7	0·026	3·3	0·018	3·8	0·002
	0·758	4·0	0·027	3·5	0·018	4·0	0·002
	0·820	4·2	0·029	3·5	0·020	4·1	0·004
	0·880	1·7	0·029	4·2	0·021	4·3	−0·004
	0·942	2·1	0·035	4·4	0·021	3·7	−0·046
0·777	0·072	2·9	−0·012	2·6	−0·015	2·8	−0·028
	0·174	2·8	−0·010	2·6	−0·012	2·9	−0·026
	0·277	2·9	−0·007	2·7	−0·012	3·0	−0·024
	0·381	3·0	−0·004	2·7	−0·007	3·1	−0·021
	0·432	3·0	−0·001	2·7	−0·004	3·0	−0·018
	0·484	3·0	0·001	2·7	−0·004	3·1	−0·018
	0·535	3·1	0·002	2·8	−0·002	3·3	−0·017
	0·588	3·3	0·004	3·0	−0·001	3·3	−0·017
	0·640	3·2	0·007	2·9	0·001	3·3	−0·013
	0·691	3·4	0·009	3·1	0·002	3·4	−0·013
	0·742	3·3	0·009	3·0	0·004	3·6	−0·012
	0·795	3·6	0·012	3·4	0·004	3·7	−0·012
	0·846	3·8	0·018	3·4	0·009	4·0	−0·009
	0·897	4·3	0·020	3·6	0·010	3·7	−0·018
	0·948	2·0	0·023	4·4	0·012	3·2	−0·040

TABLE 2

(b) 250 *ft/sec*

x/c_0	y/s_x	$\alpha = 0$ deg		$\alpha = 1$ deg		$\alpha = 2$ deg	
		$10^3\, C_f$	$+C_p$	$10^3\, C_f$	$+C_p$	$10^3\, C_f$	$+C_p$
0·333	0·104	2·7	0·035	2·7	0·023	2·8	0·012
	0·206	2·8	0·034	2·8	0·023	2·8	0·012
	0·304	2·8	0·036	2·8	0·025	3·0	0·014
	0·406	2·8	0·037	2·9	0·025	3·1	0·013
	0·504	3·2	0·038	3·2	0·026	3·1	0·014
	0·603	3·3	0·039	3·3	0·026	3·4	0·014
	0·701	3·8	0·040	3·5	0·026	3·7	0·013
	0·805	3·7	0·044	3·5	0·028	4·2	0·017
	0·901	1·7	0·046	4·1	0·031	4·2	−0·024
0·554	0·037	2·7	0·018	2·7	0·008	2·7	−0·003
	0·155	2·6	0·018	2·6	0·008	2·8	−0·002
	0·276	2·8	0·020	2·8	0·009	2·9	−0·001
	0·398	2·8	0·021	2·9	0·011	3·0	0·000
	0·458	2·8	0·022	2·8	0·011	2·9	0·000
	0·518	2·9	0·024	2·9	0·012	2·8	0·001
	0·578	2·7	0·026	2·8	0·014	3·1	0·001
	0·638	3·2	0·025	3·2	0·013	3·3	0·001
	0·699	3·2	0·027	3·1	0·015	3·6	0·004
	0·758	3·4	0·029	3·3	0·015	3·6	0·004
	0·820	3·5	0·032	3·3	0·016	3·8	0·004
	0·880	4·4	0·035	4·0	0·017	4·1	−0·009
	0·942	1·8	0·035	4·1	0·017	3·6	−0·052
0·777	0·072	2·6	−0·011	2·6	−0·019	2·6	−0·028
	0·174	2·6	−0·007	2·6	−0·017	2·7	−0·025
	0·277	2·6	−0·006	2·6	−0·015	2·8	−0·024
	0·381	2·7	−0·003	2·7	−0·012	2·9	−0·021
	0·432	2·6	0·001	2·7	−0·009	2·8	−0·018
	0·484	2·7	0·003	2·7	−0·007	2·9	−0·017
	0·535	2·8	0·003	2·8	−0·008	3·1	−0·017
	0·588	2·9	0·005	2·9	−0·007	3·1	−0·016
	0·640	2·8	0·009	2·8	−0·002	3·0	−0·012
	0·691	3·0	0·009	3·0	−0·003	3·2	−0·013
	0·742	2·9	0·012	2·9	0·000	3·3	−0·011
	0·795	3·2	0·013	3·2	0·000	3·4	−0·011
	0·846	3·3	0·018	3·1	0·004	3·8	−0·009
	0·897	3·5	0·021	3·5	0·004	3·6	−0·023
	0·948	4·4	0·026	4·0	0·005	3·0	−0·045

TABLE 2(b) (*Contd.*)

x/c_0	y/s_x	$\alpha = 4$ deg		$\alpha = 6$ deg		$\alpha = 8$ deg	
		$10^3\,C_f$	$-C_p$	$10^3\,C_f$	$-C_p$	$10^3\,C_f$	$-C_p$
0·333	0·104	3·0	0·009	2·9	0·032	3·1	0·050
	0·206	2·9	0·010	3·0	0·032	3·3	0·050
	0·304	2·9	0·008	3·4	0·030	3·4	0·047
	0·406	3·4	0·008	3·8	0·027	3·8	0·043
	0·504	3·8	0·006	3·9	0·022	4·4	0·038
	0·603	4·1	0·001	4·6	0·012	4·9	0·076
	0·701	4·6	−0·014	5·6	0·105	6·6	0·359
	0·805	5·9	0·165	6·6	0·378	4·8	0·405
	0·901	3·0	0·127	2·8	0·210	3·4	0·290
0·544	0·037	2·9	0·021	2·7	0·040	2·9	0·055
	0·155	2·7	0·021	2·8	0·041	3·1	0·055
	0·276	2·8	0·020	3·0	0·037	3·3	0·051
	0·398	3·1	0·019	3·5	0·035	3·4	0·046
	0·458	3·3	0·018	3·5	0·031	3·8	0·042
	0·518	3·4	0·015	3·8	0·025	4·2	0·038
	0·578	3·7	0·011	4·1	0·016	4·5	0·050
	0·638	4·0	0·005	4·4	0·021	5·2	0·132
	0·699	4·6	−0·009	5·1	0·098	6·4	0·327
	0·758	5·1	0·049	6·7	0·302	6·6	0·493
	0·820	5·1	0·190	5·3	0·330	3·5	0·315
	0·880	3·9	0·152	2·2	0·204	2·5	0·273
	0·942	3·1	0·123	3·7	0·199	4·2	0·270
0·777	0·072	2·6	0·042	2·8	0·054	2·8	0·063
	0·174	2·8	0·039	2·7	0·051	2·9	0·060
	0·277	2·8	0·039	2·8	0·050	3·1	0·057
	0·381	2·9	0·035	3·1	0·045	3·3	0·050
	0·432	2·9	0·031	3·2	0·040	3·4	0·043
	0·484	3·0	0·029	3·4	0·035	3·7	0·038
	0·535	3·3	0·028	3·7	0·031	3·9	0·037
	0·588	3·4	0·022	4·0	0·022	4·3	0·049
	0·640	3·8	0·012	4·5	0·017	4·7	0·113
	0·691	4·1	0·005	4·9	0·077	5·8	0·283
	0·742	5·0	0·033	5·5	0·226	6·2	0·444
	0·795	5·2	0·140	5·9	0·352	4·9	0·378
	0·846	4·4	0·178	2·9	0·207	1·8	0·246
	0·897	2·2	0·119	2·6	0·185	3·1	0·247
	0·948	3·0	0·110	3·5	0·171	3·7	0·228

TABLE 2(b) (*Contd.*)

x/c_0	y/s_x	$\alpha = 10$ deg		$\alpha = 12$ deg		$\alpha = 14$ deg	
		$10^3\,C_f$	$-C_p$	$10^3\,C_f$	$-C_p$	$10^3\,C_f$	$-C_p$
0·333	0·104	3·4	0·076	3·7	0·110	4·4	0·141
	0·206	3·5	0·076	3·9	0·110	4·7	0·145
	0·304	3·8	0·072	4·3	0·110	4·7	0·157
	0·406	4·3	0·071	4·6	0·128	5·3	0·212
	0·504	5·1	0·093	5·7	0·216	6·5	0·385
	0·603	6·4	0·255	7·7	0·506	8·4	0·750
	0·701	7·9	0·612	8·1	0·781	8·6	0·892
	0·805	4·2	0·425	3·4	0·489	3·0	0·573
	0·901	3·7	0·379	3·6	0·476	4·3	0·571
0·554	0·037	3·0	0·073	3·2	0·100	3·8	0·123
	0·155	3·3	0·073	3·5	0·099	3·8	0·124
	0·276	3·3	0·068	3·8	0·097	3·9	0·128
	0·398	3·6	0·066	4·2	0·108	4·4	0·174
	0·458	4·3	0·068	4·5	0·136	5·1	0·242
	0·518	4·4	0·090	5·2	0·216	5·7	0·381
	0·578	4·9	0·170	5·9	0·382	7·2	0·591
	0·638	6·1	0·356	7·4	0·601	7·9	0·795
	0·699	7·0	0·564	7·2	0·712	7·2	0·816
	0·758	6·0	0·565	5·5	0·600	4·8	0·637
	0·820	2·8	0·359	2·3	0·433	2·3	0·506
	0·880	2·5	0·348	2·8	0·428	2·6	0·505
	0·942	4·7	0·349	5·0	0·437	5·1	0·523
0·777	0·072	3·0	0·073	3·3	0·088	3·5	0·099
	0·174	3·0	0·069	3·2	0·084	3·6	0·097
	0·277	3·5	0·065	3·6	0·080	3·5	0·097
	0·381	3·4	0·059	3·8	0·083	4·0	0·124
	0·432	3·9	0·054	4·3	0·094	4·3	0·160
	0·484	4·0	0·059	4·2	0·129	4·9	0·237
	0·535	4·4	0·087	5·1	0·211	5·6	0·369
	0·588	5·2	0·164	6·1	0·354	6·4	0·544
	0·640	5·9	0·316	7·0	0·536	7·0	0·698
	0·691	7·1	0·512	6·7	0·663	6·9	0·747
	0·742	6·1	0·546	5·4	0·581	4·9	0·599
	0·795	3·6	0·365	2·8	0·388	2·3	0·433
	0·846	2·2	0·302	2·5	0·365	2·0	0·418
	0·897	3·2	0·311	3·7	0·376	3·7	0·432
	0·948	3·9	0·287	4·1	0·353	4·5	0·414

LIST OF SYMBOLS

x	Distance behind leading-edge apex of wing
y	Spanwise distance from centreline of wing
c_0	Root chord
s	Semi-span
s_x	Local semi-span
α	Incidence
q_0	Freestream kinetic pressure
q	Local kinetic pressure
C_p	Pressure coefficient
τ	Surface shear stress
C_f	Skin-friction coefficient, τ/q_0
C_{f_q}	Skin-friction coefficient based on local q, τ/q
C_{f_x}	Skin-friction coefficient in two-dimensional flow
R_x	Reynolds number based on distance x
F	Scaling factor
β	Flow direction relative to freestream, yaw of surface pitot-tube
C_{f_β}	Skin-friction coefficient measured by a yawed surface pitot-tube
h	Razor-blade height
Δx	Razor-blade displacement
ρ	Air density
μ	Air viscosity
Δp	Pressure difference recorded by surface pitot-tube
C, m	Calibration constants
M	Mach number

REFERENCES

No.	*Author(s)*	*Title, etc.*
1	K. G. Smith, L. Gaudet K. G. Winter ..	The use of surface pitot-tubes as skin-friction meters at supersonic speeds. A.R.C. R. & M. 3351. June 1962.
2	J. N. Hool	Measurement of skin friction using surface tubes. Aircraft Engineering *28*, 52–54. 1956.
3	L. A. Wyatt, T. B. Owen ..	Preliminary low speed measurements of skin friction and surface pressure fluctuations on a slender wing at incidence. RAE Technical Note Aero 2916. A.R.C. 25,436. September 1963.
4	V. C. Patel	Calibration of the Preston tube and limitations on its use in pressure gradients. *J.Fluid Mech. 23*, 185–208. September 1965.
5	R. J. Monaghan	Formulae and approximations for aerodynamic heating rates in high speed flight. A.R.C. C.P. 360. March 1956.

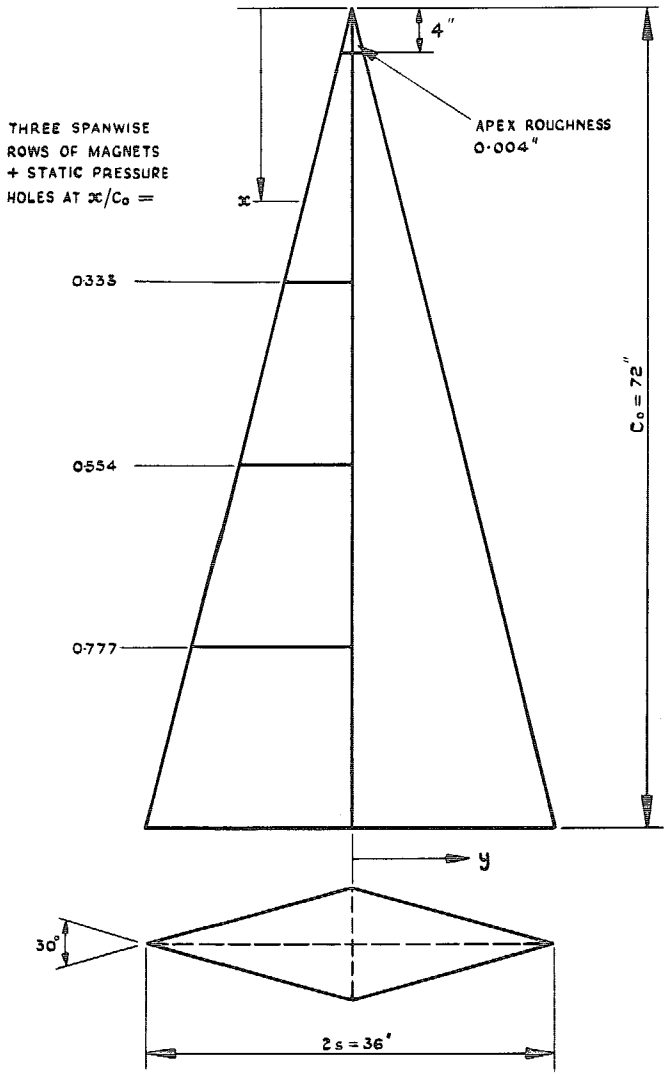

FIG. 1. General arrangement of rhombic cone.

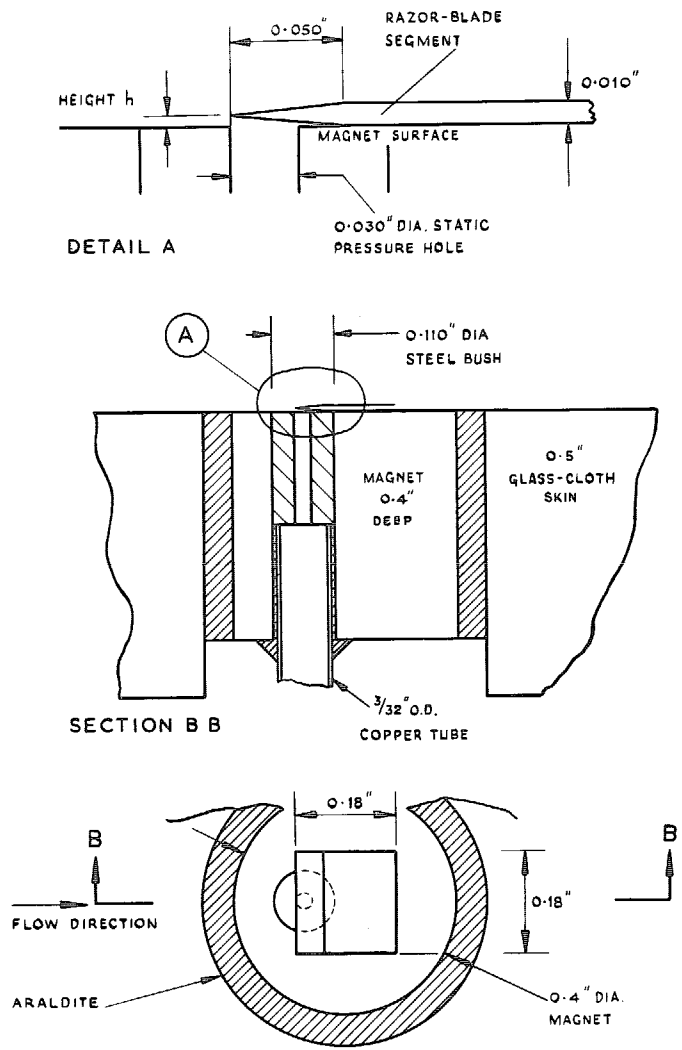

FIG. 2. Mounting of surface pitot-tube.

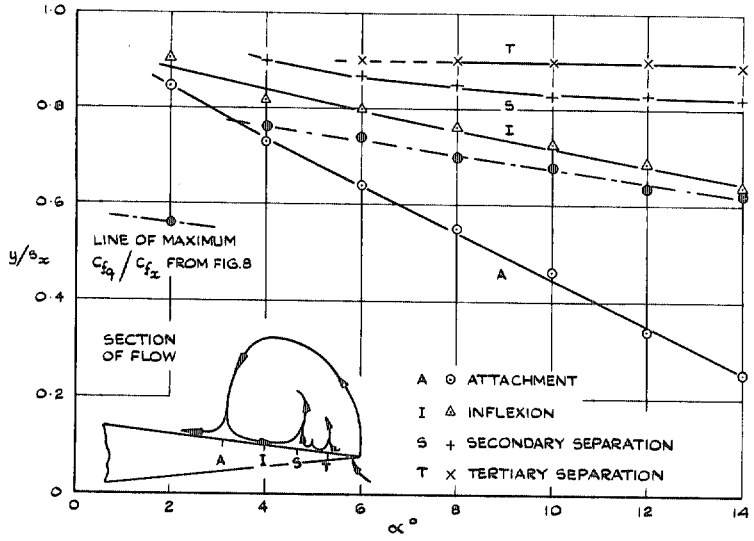

FIG. 5. Position of upper-surface flow features.

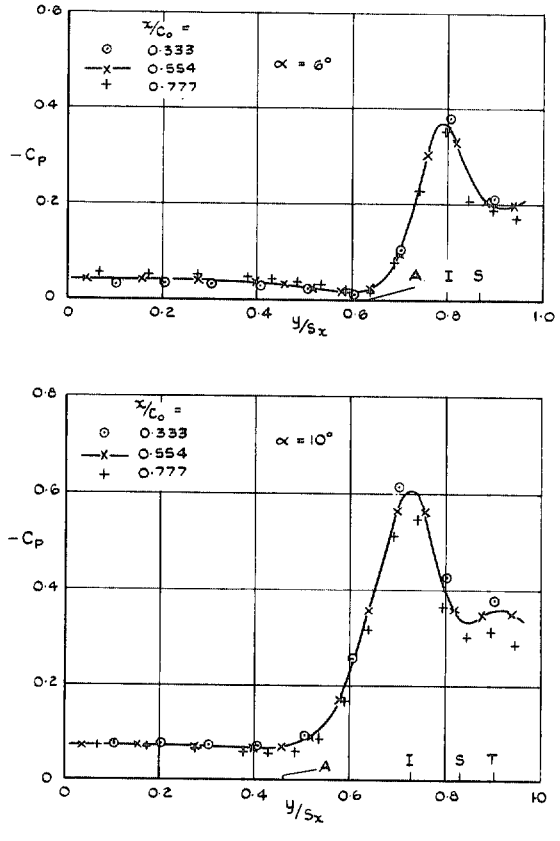

FIG. 6. Pressure distribution over upper surface $\alpha = 6$ and 10 deg. 250 ft/sec.

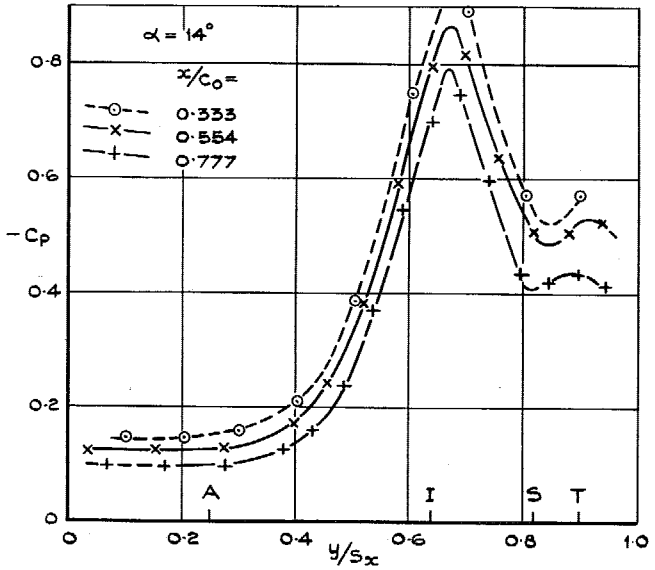

FIG. 6 (CONT'D) $\alpha = 14^\circ$

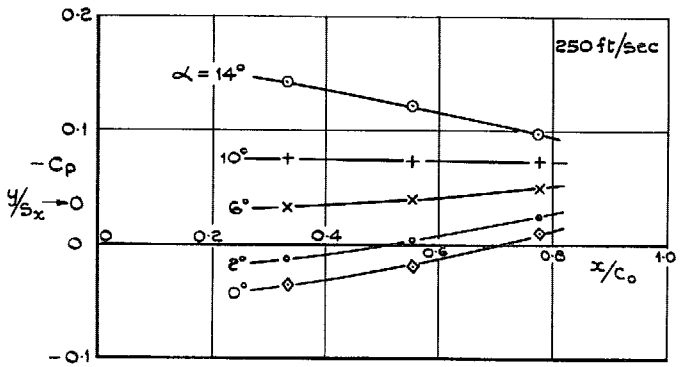

FIG. 7. Pressure distribution near centreline on upper surface.

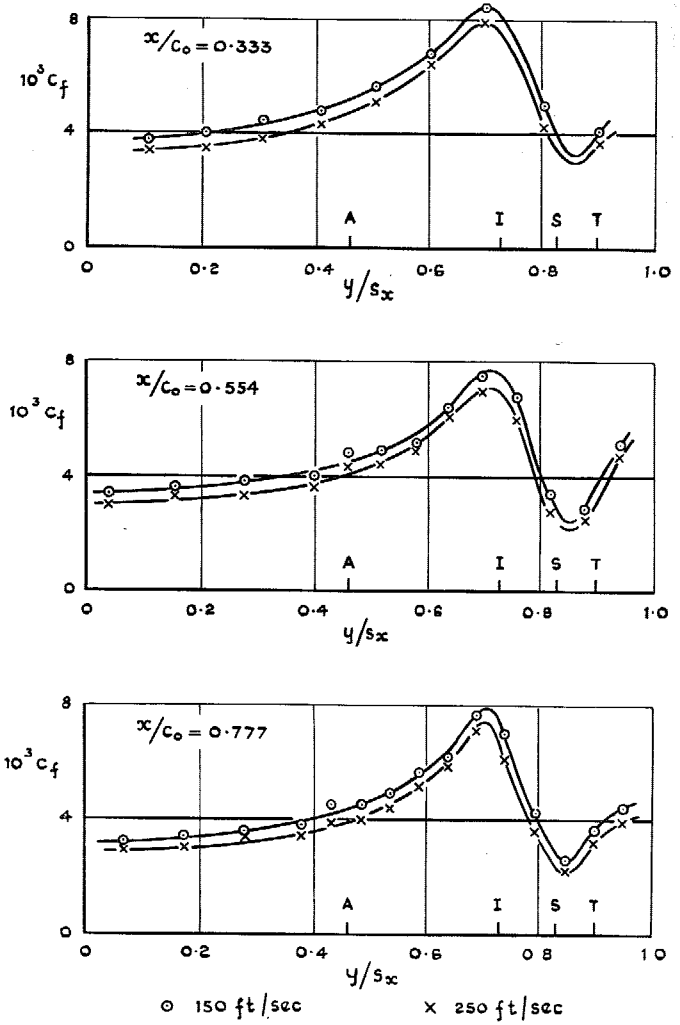

FIG. 8. Skin-friction distribution over upper surface at $\alpha = 10$ deg.

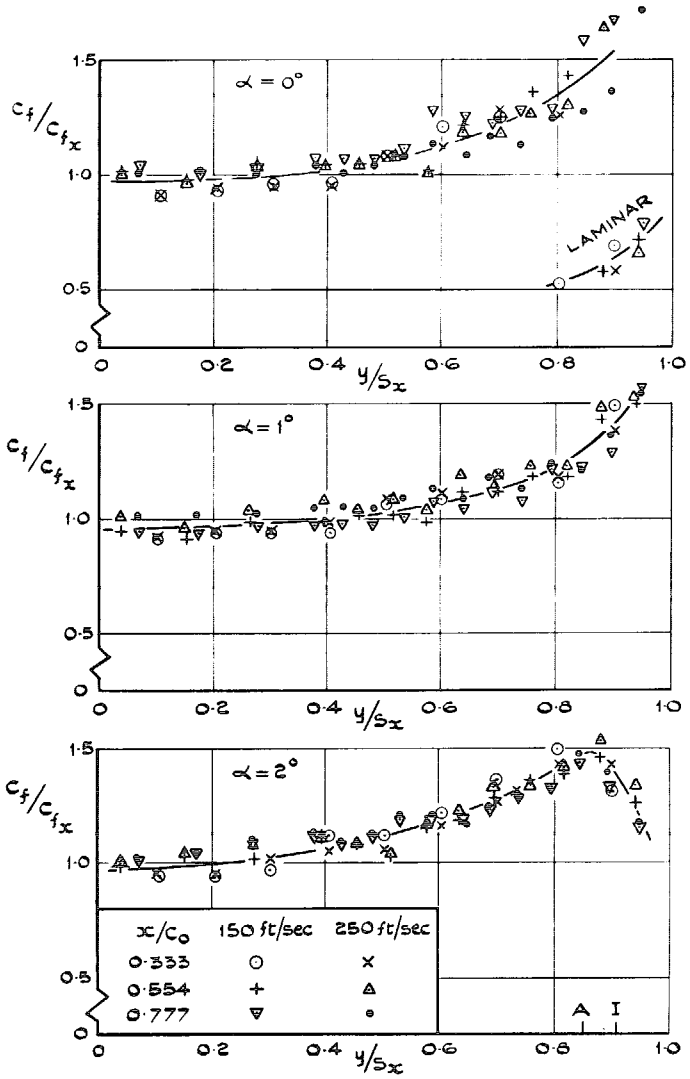

FIG. 9. Distribution of C_f/C_{f_x} over upper surface at $\alpha = 0$, 1 and 2 deg.

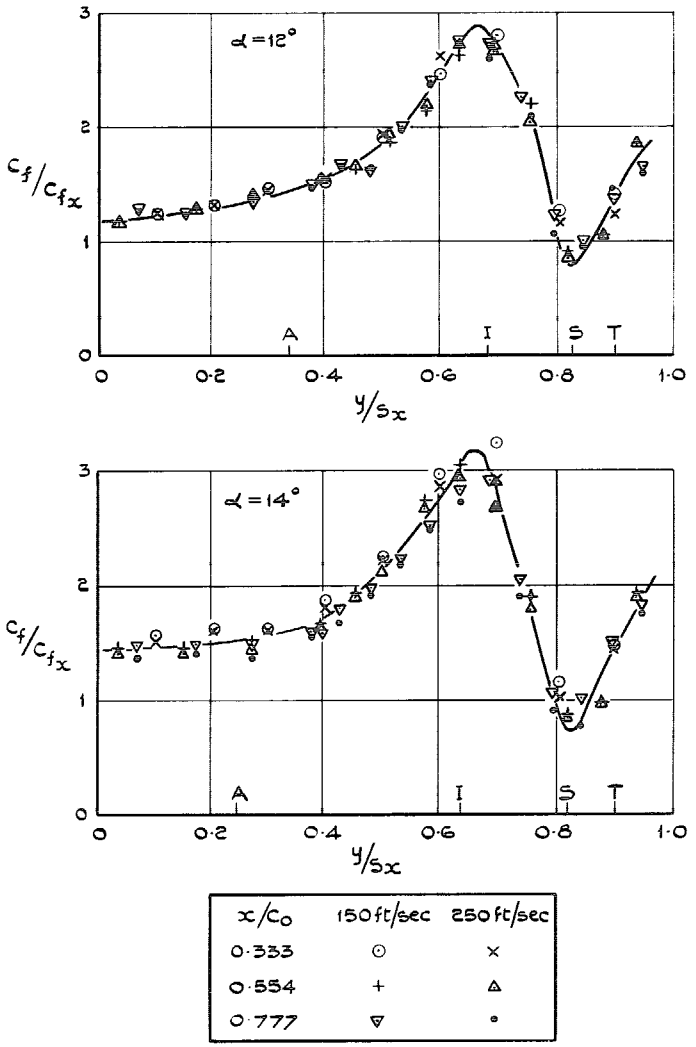

FIG. 9.(contd.). $\alpha = 12$ and 14 deg.

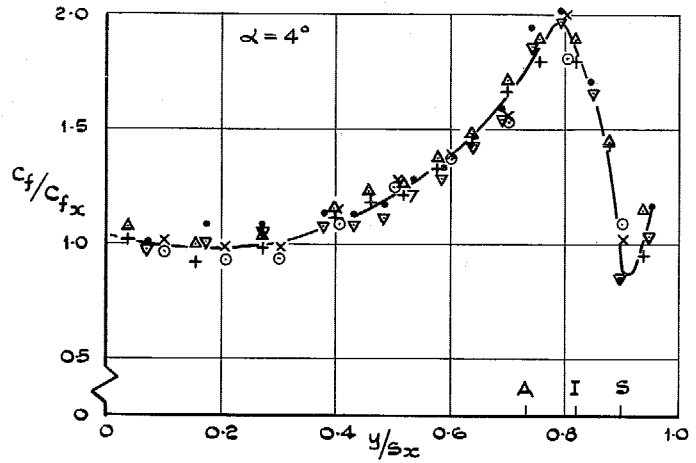

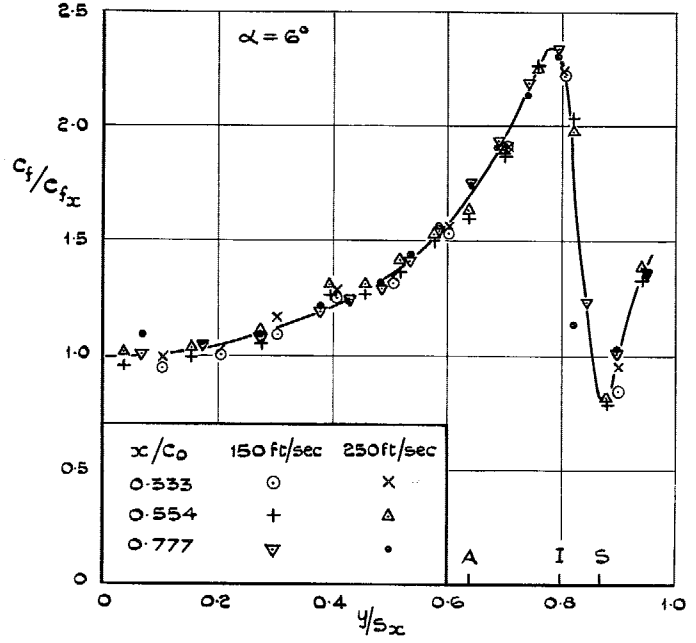

FIG. 9. (contd.). $\alpha = 4$ and 6 deg.

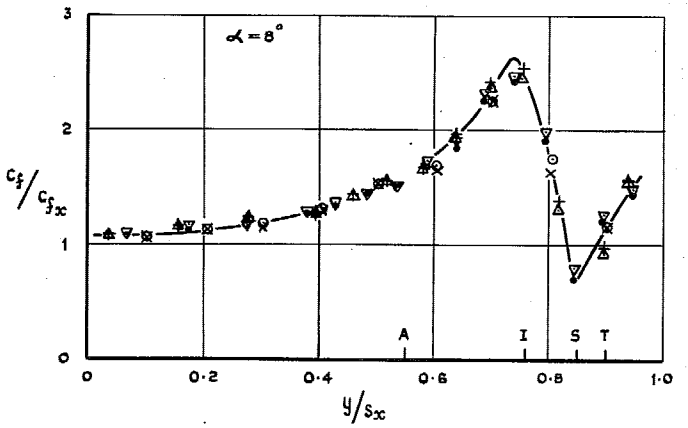

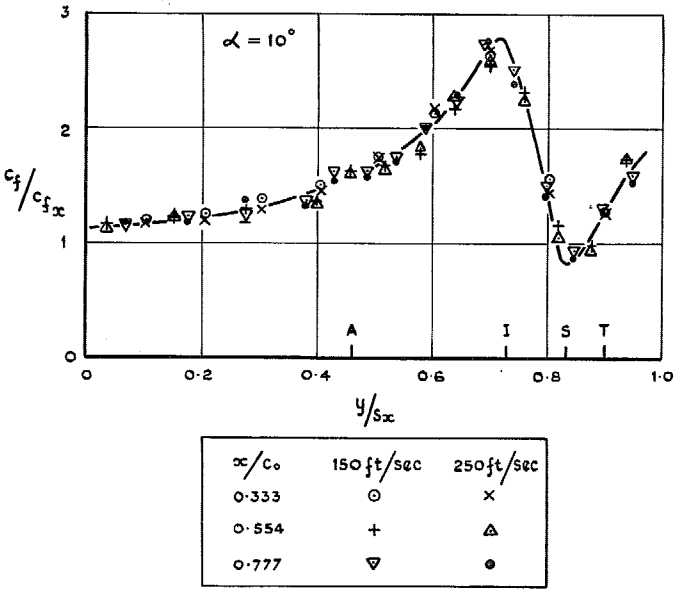

FIG. 9. (contd.). $\alpha = 8$ and 10 deg.

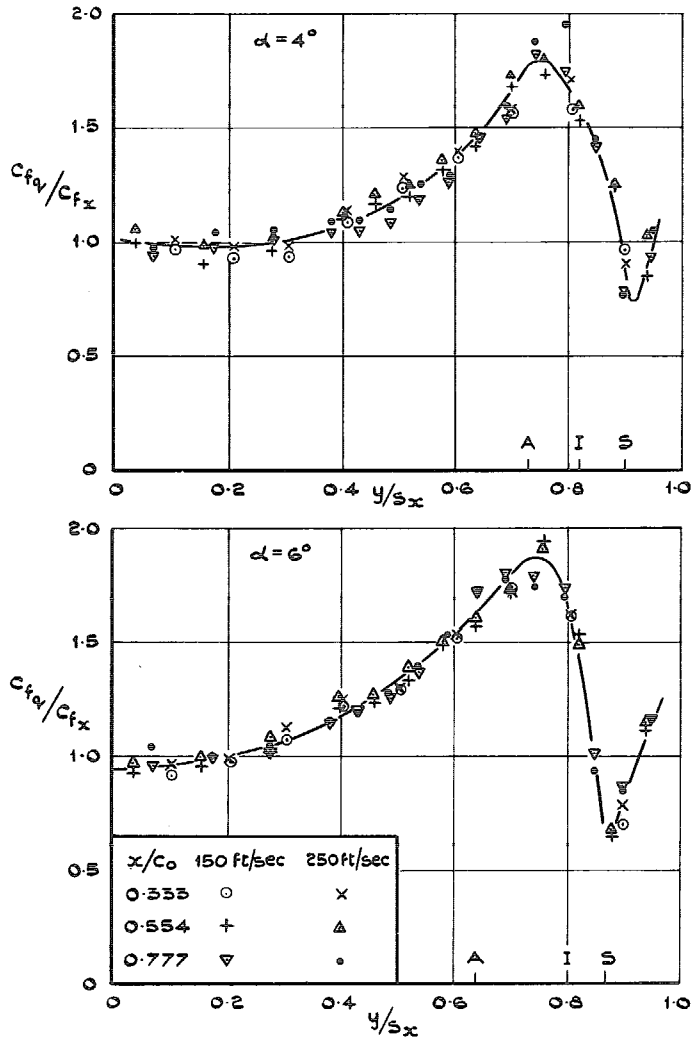

FIG. 10. Distribution of C_{fq}/C_{fx} over upper surface at $\alpha = 4$ and 6 deg.

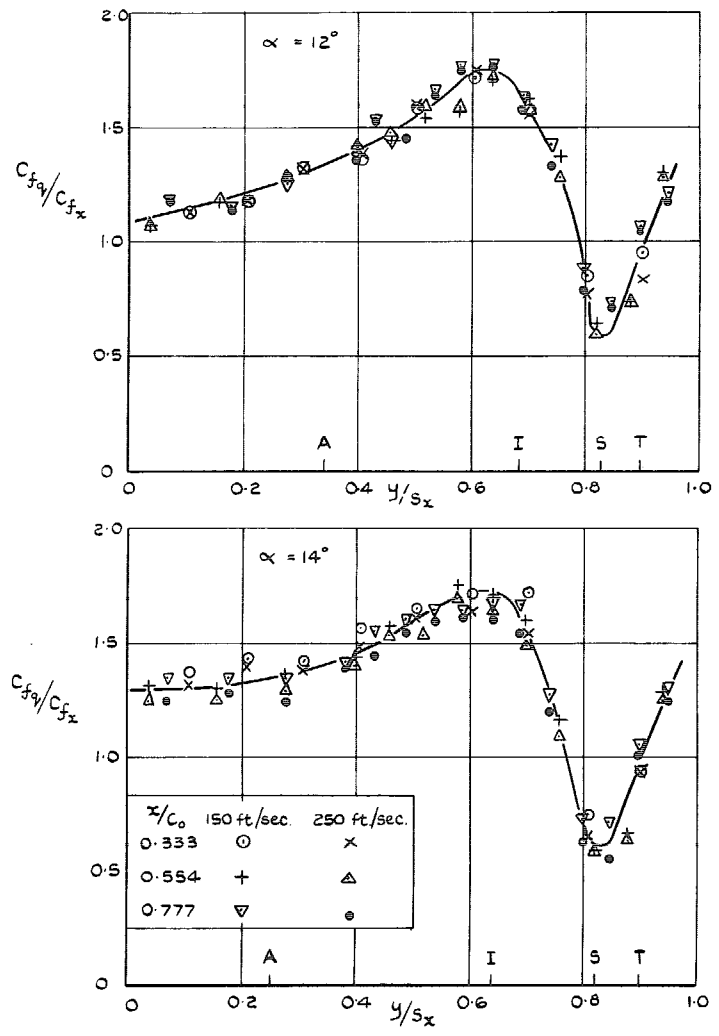

FIG. 10. (contd.). $\alpha = 12$ and 14 deg.

Dd.129527 K5.

Printed in Wales for Her Majesty's Stationery Office by Allens Printers (Wales) Limited.

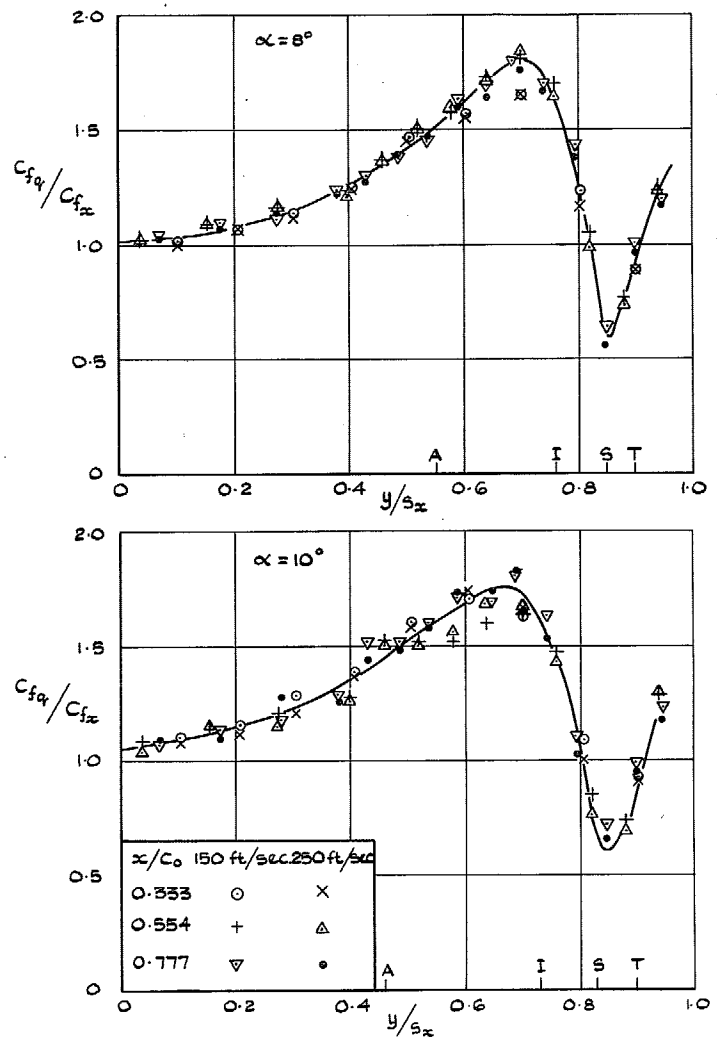

FIG. 10. (contd.). $\alpha = 8$ and 10 deg.

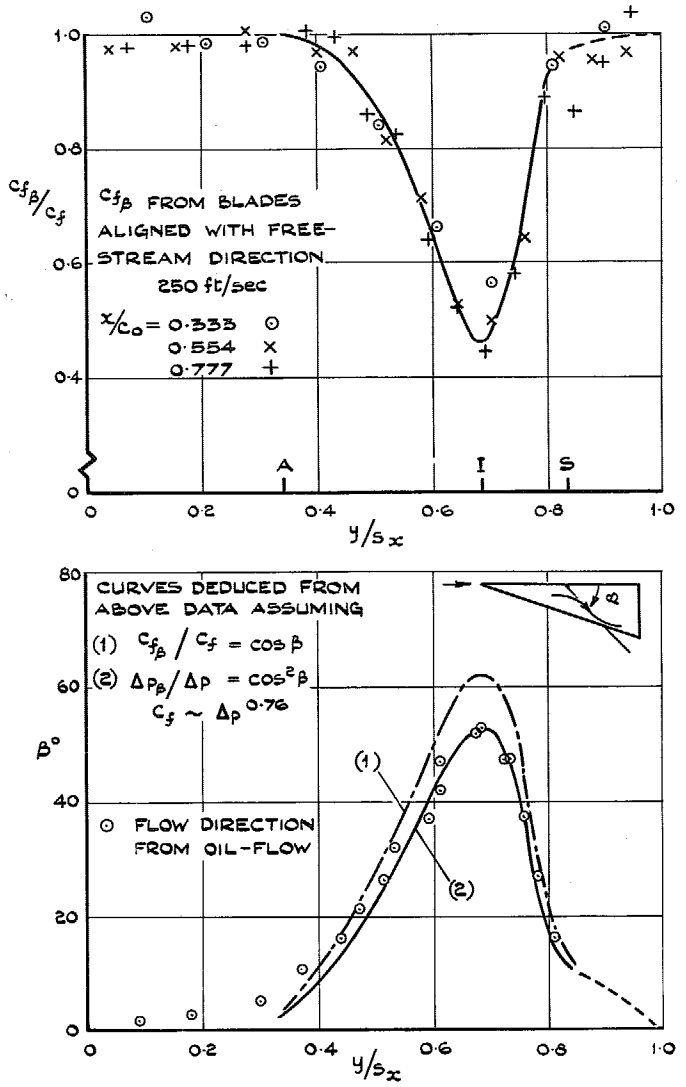

FIG. 11. Apparent skin friction, $C_{f\beta}$, in free-stream direction and deduced flow direction, β, at $\alpha = 12$ deg.

Published by
HER MAJESTY'S STATIONERY OFFICE

To be purchased from
49 High Holborn, London W.C.1
423 Oxford Street, London W.1
13A Castle Street, Edinburgh 2
109 St. Mary Street, Cardiff CF1 1JW
Brazennose Street, Manchester 2
50 Fairfax Street, Bristol 1
258 259 Broad Street, Birmingham 1
7 11 Linenhall Street, Belfast BT2 8AY
or through any bookseller

R. & M. No. 3499

S.O. Code No. 23 3499